

Channel Coding Diversity with Mismatched Decoding Metrics

Trung Thanh Nguyen, *Student Member, IEEE*, and Lutz Lampe, *Senior Member, IEEE*

Abstract—We analyze the performance of channel coding diversity with general decoding metrics in terms of the generalized mutual information (GMI). We show that the GMI of the diversity channel is less than or equal to the baud-rate weighted sum of the component GMIs; and equality is achieved only in special cases. We then focus on bit-interleaved coded modulation (BICM) schemes and demonstrate the applicability of our findings by an example of hybrid free-space optical and radio-frequency (FSO-RF) communication.

Index Terms—Channel coding diversity, mismatched decoding, generalized mutual information (GMI), bit-interleaved coded modulation (BICM), symbol-by-symbol (SBS) decoding.

I. INTRODUCTION

Channel coding diversity (CCD) refers to the use of parallel channels to transmit the same coded information. It is a promising solution to combat fluctuations in the quality of individual channels while simultaneously utilizing all available channel resources [1]. An interesting example is bit-interleaved coded modulation (BICM) with hybrid free-space optical and radio-frequency (FSO-RF) transmission for last-mile access, e.g. [2]. Such hybrid systems enable high-rate communication in a wide variety of weather-induced fading scenarios where the quality of a single (either FSO or RF) channel could be severely degraded.

In this letter, we consider CCD with approximate (mismatched) decoding metrics, which are often employed in practice to reduce detection complexity. We use the generalized mutual information (GMI) [3], [4] as the pertinent measure for achievable rates. We apply the GMI framework recently developed for BICM with mismatched decoding metrics in [5]–[7], and show the interesting result that the GMI of the overall *diversity channel* may not be the same as the baud-rate weighted sum of component channel GMIs. We demonstrate the applicability of our analysis with a relevant example of BICM-based CCD over hybrid FSO-RF transmission.

II. CHANNEL CODING DIVERSITY AND GMI

We consider the case of two parallel channels in the following, but our results can be easily generalized to other cases with more component channels. The block diagram of a CCD scheme with two component channels is presented in Figure 1. At the transmitter, a single encoder E produces a coded message, which is then mapped (or modulated) by two mappers into transmit symbols for the two component channels. At the receiver, two detectors (or demodulators) produce symbol metrics from the corresponding received symbols. A

single decoder D makes decoding decisions based on these symbol metrics.

We consider independent discrete-time memoryless component channels with input random variable $X_i \in \mathcal{X}_i$, input distribution $p_{X_i}(x_i)$, output random variable $Y_i \in \mathcal{Y}_i$, and channel transition probability function $p_{Y_i|X_i}(y_i|x_i)$, for $i = 1, 2$. The detectors produce symbol metrics of the general form $q_{X_i, Y_i}(x_i, y_i)$ with $q_{X_i, Y_i}(x_i, y_i) > 0 \forall x_i \in \mathcal{X}_i$ and $y_i \in \mathcal{Y}_i$. Let us consider a codebook \mathcal{C} of M codewords $\mathbf{x} = [\mathbf{x}^{(1)} \ \mathbf{x}^{(2)}]$. The part $\mathbf{x}^{(i)} = [x_0^{(i)} \dots x_{N_i-1}^{(i)}]$ is a length- N_i sub-codeword whose elements are to be transmitted via channel i . Let $N = N_1 + N_2$ and $\eta_i = N_i/N$. The ratio η_i is hence proportional to the baud rate¹ of channel i . Let the received sequence be $\mathbf{y} = [\mathbf{y}^{(1)} \ \mathbf{y}^{(2)}]$, where $\mathbf{y}^{(i)} = [y_0^{(i)} \dots y_{N_i-1}^{(i)}]$ comes from channel i . Given a received sequence, a word metric can be calculated for each possible codeword $\mathbf{x} \in \mathcal{C}$ as

$$q_{\mathbf{X}, \mathbf{Y}}(\mathbf{x}, \mathbf{y}) = \prod_{i=1}^2 \prod_{k=0}^{N_i-1} q_{X_i, Y_i}(x_k^{(i)}, y_k^{(i)}) . \quad (1)$$

The decoder D makes decision based on the rule

$$\hat{\mathbf{x}} = \underset{\mathbf{x} \in \mathcal{C}}{\operatorname{argmax}} q_{\mathbf{X}, \mathbf{Y}}(\mathbf{x}, \mathbf{y}) . \quad (2)$$

Following [8, Ch. 5], [3, Sec. 2], [5, Sec. 3.1.2], the word error probability, averaged over all codewords and random codebook realizations, is upper bounded as

$$P \leq M^\rho \times \prod_{i=1}^2 \mathcal{E}_{X_i, Y_i} \left\{ \left(\sum_{x'_i \in \mathcal{X}_i} p_{X_i}(x'_i) \left[\frac{q_{X_i, Y_i}(x'_i, Y_i)}{q_{X_i, Y_i}(X_i, Y_i)} \right]^s \right)^\rho \right\}^{N_i} , \quad (3)$$

(notation $\mathcal{E}(\cdot)$ denotes expectation) for all $0 \leq \rho \leq 1$ and $s > 0$. The above equation can be written as

$$P \leq 2^{-NE^r(R)} , \quad (4)$$

with rate $R \triangleq \frac{\log M}{N}$ (notation $\log(\cdot)$ denotes base-2 logarithm), the random coding exponent

$$E^r(R) \triangleq \max_{0 \leq \rho \leq 1} \max_{s > 0} (E^0(\rho, s) - \rho R) , \quad (5)$$

and the generalized Gallager function of the diversity channel

$$E^0(\rho, s) \triangleq \eta_1 E_{q_{X_1, Y_1}}^0(\rho, s) + \eta_2 E_{q_{X_2, Y_2}}^0(\rho, s) . \quad (6)$$

In (6), $E_{q_{X_i, Y_i}}^0(\rho, s)$, $i = 1, 2$, is the generalized Gallager function of the component channel i , which is defined as

The authors are with the Department of Electrical and Computer Engineering, The University of British Columbia, Vancouver, BC, Canada (email: {trungn, lampe}@ece.ubc.ca).

¹Or symbol rate, which is the inverse of the symbol period.

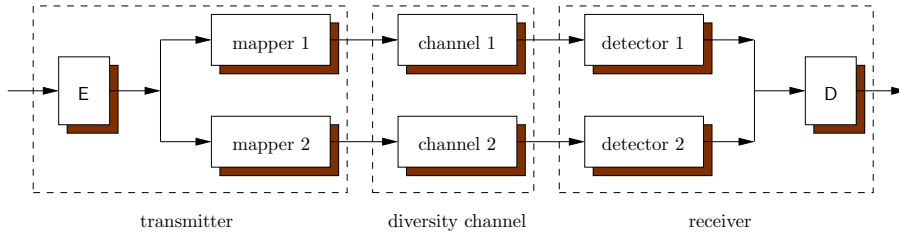


Fig. 1. A channel coding diversity scheme with two parallel component channels.

$$E_{q_{X_i, Y_i}}^0(\rho, s) \triangleq -\log \mathcal{E}_{X_i, Y_i} \left\{ \left(\sum_{x'_i \in \mathcal{X}_i} p_{X_i}(x'_i) \left[\frac{q_{X_i, Y_i}(x'_i, Y_i)}{q_{X_i, Y_i}(X_i, Y_i)} \right]^s \right)^\rho \right\} \quad (7)$$

The GMI is the supremum of all rates for which P vanishes with increasing N according to (4). It is a popular measure of achievable rates for mismatched decoding. In particular, the GMI is defined as

$$I^{\text{gmi}} \triangleq \max_{s>0} I(s), \quad (8)$$

with

$$I(s) \triangleq \left. \frac{\partial E^0(\rho, s)}{\partial \rho} \right|_{\rho=0} = \lim_{\rho \rightarrow 0} \frac{E^0(\rho, s)}{\rho} = \eta_1 I_{q_{X_1, Y_1}}(s) + \eta_2 I_{q_{X_2, Y_2}}(s) \quad (9)$$

and

$$I_{q_{X_i, Y_i}}(s) = -\mathcal{E}_{X_i, Y_i} \left\{ \log \sum_{x'_i \in \mathcal{X}_i} p_{X_i}(x'_i) \left[\frac{q_{X_i, Y_i}(x'_i, Y_i)}{q_{X_i, Y_i}(X_i, Y_i)} \right]^s \right\}. \quad (10)$$

The function $I_{q_{X_i, Y_i}}(s)$ is the I-curve of the component channel i [7], and accordingly, we refer to $I(s)$ in (9) as the I-curve of the diversity channel. The GMI of the component channel i is the peak value of the I-curve $I_{q_{X_i, Y_i}}(s)$,

$$I_{q_{X_i, Y_i}}^{\text{gmi}} \triangleq \max_{s>0} I_{q_{X_i, Y_i}}(s). \quad (11)$$

Interestingly, from (8), (9), and (11), it follows that

$$\begin{aligned} I^{\text{gmi}} &= \max_{s>0} (\eta_1 I_{q_{X_1, Y_1}}(s) + \eta_2 I_{q_{X_2, Y_2}}(s)) \\ &\leq \eta_1 \max_{s>0} I_{q_{X_1, Y_1}}(s) + \eta_2 \max_{s>0} I_{q_{X_2, Y_2}}(s) \\ &= \eta_1 I_{q_{X_1, Y_1}}^{\text{gmi}} + \eta_2 I_{q_{X_2, Y_2}}^{\text{gmi}}. \end{aligned}$$

That is, the GMI of the diversity channel is less than or equal to the baud-rate weighted sum of the component channel GMIs. Equality

$$I^{\text{gmi}} = \eta_1 I_{q_{X_1, Y_1}}^{\text{gmi}} + \eta_2 I_{q_{X_2, Y_2}}^{\text{gmi}} \quad (12)$$

holds if and only if the individual I-curves attain their peaks at the same value of s , cf. [7, Theorem 1]. This is the case if, for example, $q_{X_i, Y_i}(x_i, y_i)$, $\forall i$, are matched metrics for which the individual I-curves peak at $s = 1$ [8]. Metric $q_{X_i, Y_i}(x_i, y_i)$ is a matched metric if it is proportional to the corresponding channel transition probability function $p_{Y_i|X_i}(y_i|x_i)$.

Remark: We would like to compare CCD with BICM. Eqn. (9) shows how the I-curve of the CCD channel can be decomposed into a weighted sum of the component I-curves. If we model BICM as comprising of independent binary-input channels [9, Sec. II-C.3], then BICM becomes a special case of CCD where the component channels have the same baud rate and the same received samples. Interestingly, the I-curve decomposition for BICM [7, Eqn. (19)] can then be obtained directly from (9) (with an appropriate adjustment to the unit of the GMI: if a factor $1/m$ is multiplied to the right hand side of [7, Eqn. (19)], the unit of the GMI would be bits per binary channel use). We note that the I-curve decomposition for BICM was first shown in [6] for the uniform input distribution and later extended in [7] for general input distribution.

III. NUMERICAL EXAMPLE AND DISCUSSION

In this section we use a numerical example to demonstrate the applicability of our analytical result.

A. Setup

Let us consider a hybrid FSO-RF transmission similar to the one in [2]. It is a BICM-based CCD system where (E, D) in Figure 1 is a binary encoder-decoder pair, and channel 1 and 2 are an FSO and an RF channel. Each branch from mapper i to detector i is similar to an ordinary BICM system. That is, given a received sample y_i , detector i produces a log-likelihood ratio (LLR) $\Lambda_{q_{B_j, Y_i}}(y_i)$ for each labeling bit position j . We consider uniform input for which the binary I-curve for each bit position can be estimated by Monte-Carlo integration according to [7, Eqn. (18)]

$$I_{q_{B_j, Y_i}}(s) = 1 - \mathcal{E}_{X_i, Y_i} \left\{ \log_2(1 + \exp(-\text{sgn}(b_j(X_i)) \Lambda_{q_{B_j, Y_i}}(Y_i)s)) \right\}, \quad (13)$$

where $b_j(X_i)$ is the j -th bit in the label of X_i and $\text{sgn}(\cdot)$ is defined as $\text{sgn}(0) = 1$ and $\text{sgn}(1) = -1$. The I-curve of channel i is the sum of the binary I-curves in that channel, according to [6], [7, Eqn. (19)]. The RF channel uses 64-QAM with max-log LLR, symbol period of $T_{\text{RF}} = 60$ ns, and block fading. We assume a signal-to-noise ratio (SNR) such that the BICM GMI (11) is equal to 2.0 bits per channel use (bpcu). The FSO channel uses 64-ary pulse-position modulation (64-PPM) with symbol period of $T_{\text{FSO}} = 40$ ns. The photon-counting channel model [10] with background radiation of 2.44 photons/slot is applied. This background radiation value is compatible with a terrestrial FSO scenario [11]. We also

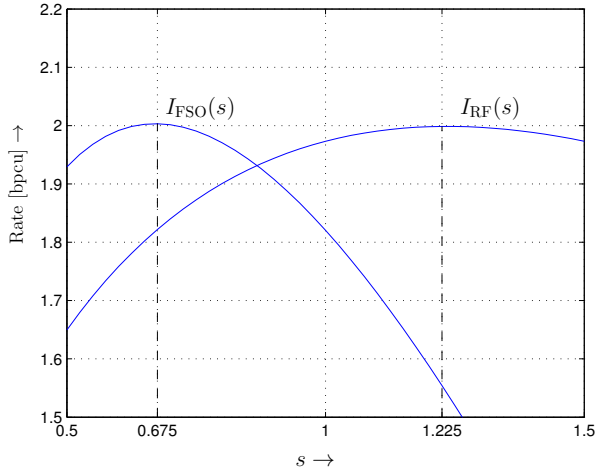


Fig. 2. BICM I-curves of component channels.

use the max-log LLR metric for PPM, see [7, Sec. IV-B], and assume a signal radiation level which makes the BICM GMI (11) of the FSO channel also equal to 2.0 bpcu. The BICM I-curves of the FSO and RF component channels are shown in Figure 2. We see that they attain their peaks at different values of s ($s = 0.675$ for the FSO I-curve $I_{\text{FSO}}(s)$ and $s = 1.225$ for the RF I-curve $I_{\text{RF}}(s)$).

B. CCD GMI

We now apply our analysis in Section II to estimate the GMI of the diversity channel. We have $\eta_{\text{FSO}} = (1/T_{\text{FSO}})/(1/T_{\text{FSO}} + 1/T_{\text{RF}}) = 0.6$. Similarly, $\eta_{\text{RF}} = 0.4$. From (9), the I-curve of the diversity channel is

$$I(s) = 0.6I_{\text{FSO}}(s) + 0.4I_{\text{RF}}(s), \quad (14)$$

and is plotted in Figure 3. This I-curve peaks at $s = 0.775$ and attains a GMI of only 1.94 bpcu and the equality (12) does not hold.

We can apply the LLR scaling technique from [7] to align the two component I-curves. That is, if we scale all the FSO LLR values by 0.675 and all the RF LLR values by 1.225 (all LLR values of the same channel are scaled by the same constant, regardless of the bit position), the s -coordinate of the peaks of the FSO and RF I-curves are shifted to $s = 1$. Now, the larger GMI value of 2.0 bpcu is achieved for the diversity channel and equality (12) holds. The corresponding I-curve of the diversity channel $I_{\text{scaled}}(s)$ is also plotted in Figure 3.

To demonstrate that our GMI analysis actually reflects the performance of coded transmission, we use the Raptor code as described in [7, Example 1] and sum-product symbol-by-symbol decoding for the hybrid FSO-RF transmission. The throughput achieved by this coded system without and with metric scaling is plotted as markers below the corresponding I-curves in Figure 3. It can be seen that the simulated throughput follows the corresponding GMI value, with 1.75 bpcu and 1.85 bpcu for transmission without and with metric scaling, respectively. Since metric scaling can be easily implemented (with an SNR-dependent scaling factor; however, SNR information is

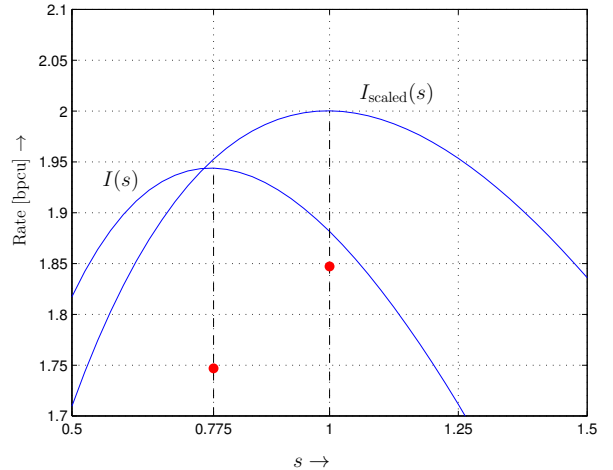


Fig. 3. BICM I-curve and coded throughput of the diversity channel.

often available and used at the receiver for detection anyhow), it is a practical approach to improve the performance of CCD.

IV. CONCLUSION

We have studied CCD with general decoding metrics, applying the GMI as the relevant performance measure. We have shown that the GMI of the diversity channel may be smaller than the sum of baud-rate weighted GMIs of individual channels. We have also illustrated the applicability of our approach by an example of hybrid FSO-RF transmission using suboptimal max-log decoding metrics.

REFERENCES

- [1] J. N. Laneman, E. Martinián, G. W. Wornell, and J. G. Apostolopoulos, "Source-channel diversity for parallel channels," *IEEE Trans. Inf. Theory*, vol. 51, no. 10, pp. 3518–3539, 2005.
- [2] A. AbdulHussein, A. Oka, T. T. Nguyen, and L. Lampe, "Rateless coding for hybrid free-space optical and radio-frequency communication," *IEEE Trans. Wireless Commun.*, vol. 9, no. 3, pp. 907–913, Mar. 2010.
- [3] G. Kaplan and S. Shamai, "Information rates and error exponents of compound channels with application to antipodal signaling in a fading environment," *Archiv Elektronik Übertragungstechnik (AEÜ)*, vol. 47, no. 4, pp. 228–239, 1993.
- [4] N. Merhav, A. Lapidoth, and S. Shamai, "On information rates for mismatched decoders," *IEEE Trans. Inf. Theory*, vol. 40, no. 6, pp. 1953–1967, 1994.
- [5] A. Guillén i Fàbregas, A. Martínez, and G. Caire, "Bit-interleaved coded modulation," *Found. Trends Commun. Inf. Theory*, vol. 5, no. 1-2, pp. 1–135, 2008.
- [6] A. Martínez, A. Guillén i Fàbregas, G. Caire, and F. Willems, "Bit-interleaved coded modulation revisited: A mismatched decoding perspective," *IEEE Trans. Inf. Theory*, vol. 55, no. 6, Jun. 2009.
- [7] T. T. Nguyen and L. Lampe, "Bit-interleaved coded modulation with mismatched decoding metrics," *IEEE Trans. Commun.*, vol. 59, no. 2, pp. 437–447, Feb. 2011.
- [8] R. G. Gallager, *Information Theory and Reliable Communication*. New York, NY: Wiley, 1968.
- [9] G. Caire, G. Taricco, and E. Biglieri, "Bit-interleaved coded modulation," *IEEE Trans. Inf. Theory*, vol. 44, pp. 927–946, May 1998.
- [10] S. J. Dolinar, J. Hamkins, B. E. Moision, and V. A. Vlnrotter, "Optical modulation and coding," in *Deep Space Optical Communications*, H. Hemmati, Ed. Wiley-Interscience, Apr. 2006.
- [11] S. G. Wilson, M. Brandt-Pearce, Q. Cao, and J. H. Leveque, "Free-space optical MIMO transmission with Q-ary PPM," *IEEE Trans. Commun.*, vol. 53, no. 8, pp. 1402–1412, 2005.